Available online at www.sciencedirect.com
ScienceDirect
Journal of Solid State Chemistry 181 (2008) 611–615
JOURNAL OF SOLID STATE CHEMISTRY
www.elsevier.com/locate/jssc

Neutron powder diffraction study of the crystal and magnetic structures of $BiNiO_3$ at low temperature

Sandra J.E. Carlsson[a], Masaki Azuma[b], Yuichi Shimakawa[b], Mikio Takano[b], Alan Hewat[c], J. Paul Attfield[a,*]

[a]*Centre for Science at Extreme Conditions, University of Edinburgh, Erskine Williamson Building, King's Buildings, Mayfield Road, Edinburgh EH9 3JZ, UK*
[b]*Institute for Chemical research, Kyoto University, Uji, Kyoto-fu 611 0011, Japan*
[c]*Institut Laue et Langevin, Grenoble, France*

Received 17 October 2007; received in revised form 20 December 2007; accepted 22 December 2007
Available online 9 January 2008

Abstract

The crystal and magnetic structures of the charge ordered perovskite $BiNiO_3$ have been studied at temperatures from 5 to 300 K using neutron diffraction. Rietveld analysis of the data shows that the structure remains triclinic (space group $P\bar{1}$) throughout the whole temperature range. Bond-valence sum calculations based on the Bi–O and Ni–O bond distances confirm that the charge distribution is $Bi^{3+}_{0.5}Bi^{5+}_{0.5}Ni^{2+}O_3$ down to 5 K. The magnetic cell is identical to that of the triclinic superstructure and a *G*-type antiferromagnetic model gives a good fit to the magnetic intensities, with an ordered Ni^{2+} moment of 1.76(3) μ_B at 5 K. However, $BiNiO_3$ is ferrimagnetic due to the inexact cancellation of opposing, inequivalent moments in the low symmetry cell.
© 2008 Elsevier Inc. All rights reserved.

Keywords: Magnetic structure; Neutron diffraction; Perovskite oxides

1. Introduction

Transition metal oxides with the perovskite structure display a wide variety of interesting properties such as magnetism, high-T_c superconductivity and colossal magnetoresistances. The $RNiO_3$ perovskites (R = rare earth) are an interesting family of compounds which, except for $R = La$, show a metal-insulator phase transition with decreasing temperature [1,2]. A partial $2Ni^{3+} \rightarrow Ni^{2+} + Ni^{4+}$ charge disproportionation is observed in the insulating phase. The transition temperature (T_{MI}) is strongly related to the degree of structural distortion and as the size of R decreases, the Ni–O–Ni bond angle, which determines the degree of overlapping of the Ni 3*d* and O 2*p* orbitals, becomes smaller [3] and T_{MI} is increased. The insulating $RNiO_3$ phases exhibit complex antiferromagnetic order [4,5] and the magnetic ordering temperature (T_N) coincides with T_{MI} for the larger R-cations (Pr and Nd), but diverges below T_{MI} with increasingly smaller R.

$BiNiO_3$ has very different electronic properties to the rare earth based nickelates, as reported previously [6,7]. Bond valence calculations based on powder synchrotron X-ray and neutron diffraction data show that the oxidation state distribution of $BiNiO_3$ is $Bi^{3+}_{0.5}Bi^{5+}_{0.5}Ni^{2+}O_3$ with the Bi charge disproportionation on the A-sites being unique for a perovskite. The charge disproportionation is suppressed by a pressure of 3–4 GPa or substitution of the A-site cation with La [8–10]. With pressure, a structural transition from the triclinic $P\bar{1}$ (insulating) to an orthorhombic *Pbnm* (metallic) phase takes place. The melting of the charge order leads to a charge transfer from Ni to Bi and the electronic state of the metallic phase can be described $Bi^{3+}Ni^{3+}O_3$. This novel transition demonstrates that $BiNiO_3$ has deep (low lying in energy) Bi:6*s* as well as deep Ni:3*d* states, comparable in energy to the O:2*p* band.

Magnetic susceptibility measurements showed that the ambient pressure phase is magnetically ordered below 300 K and a negative Weiss constant ($\theta = -262$ K)

*Corresponding author. Fax: +44 131 650 4743.
E-mail address: j.p.attfield@ed.ac.uk (J.P. Attfield).

0022-4596/$ - see front matter © 2008 Elsevier Inc. All rights reserved.
doi:10.1016/j.jssc.2007.12.037

indicated that the dominant spin–spin interactions were antiferromagnetic. The Curie constant ($C=1.05\,\text{emu K mol}^{-1}$) was close to that expected ($1.00\,\text{emu K mol}^{-1}$) for $S=1$ Ni^{2+}, in keeping with the structural data. Hysteresis in the M–H data revealed a small ferromagnetic component to the magnetic order. As a continuation of the work to characterise $BiNiO_3$, we have performed neutron diffraction studies at low temperatures to determine the magnetic structure and to find whether the unusual valence distribution changes.

2. Experimental

Polycrystalline $BiNiO_3$ was obtained by high-pressure synthesis at a pressure of 6 GPa with $KClO_4$ as an oxidising agent as reported previously [6]. The 3 g sample was contained in a cylindrical vanadium can and neutron powder diffraction data were collected at 5, 100, 200 and 300 K using the constant wavelength instrument Super-D2B at the Institut Laue Langevin, Grenoble. This instrument features a bank of 128 collimated, linear-wire, position sensitive detectors separated by 1.25°, stepped in 0.05 intervals. The wavelength was $\lambda = 2.39$ Å and diffraction data in angular range $10 \leqslant 2\theta \leqslant 150°$ were analysed by Rietveld [11] method using the GSAS [12] suite of programs.

3. Results and discussion

The powder neutron diffraction patterns showed $BiNiO_3$ to be the main phase present, with an additional contribution from NiO, including a prominent cubic-$(\frac{111}{222})$ magnetic superstructure peak at $2\theta \sim 29°$ (Fig. 1(a)). No structural transitions were observed on cooling $BiNiO_3$ to 5 K and all the diffraction patterns were fitted well by refining the previously published room temperature structural model in space group $P\bar{1}$. The coordinates of the two Bi, four Ni and six distinct O sites were refined independently. Isotropic temperature U-factors were used for each atom type. The background was modelled with a linear interpolation function and the peak shape was described by a pseudo-Voigt function. The crystal and magnetic structures of the secondary phase were also fitted, showing that 5.04(7)% NiO is present.

The intensities of the $0\,\bar{1}\,1$, $0\,1\,1$, $1\,0\,\bar{1}$ and $1\,0\,1$ reflections were considerably underestimated by fitting only a nuclear model for $BiNiO_3$, with the differences increasing with decreasing temperature showing that these are magnetic Bragg contributions. No additional magnetic peaks were observed in any of the diffraction profiles indicating that the magnetic unit cell is the same as that of the structural supercell. The above reflections are derived by splitting the cubic-$(\frac{111}{222})$ perovskite reflection, showing that the magnetic order is antiferromagnetic G-type with antiparallel order of all neighbouring Ni^{2+} moments. A G-type model (Fig. 2), in which the spins on sites Ni1 and Ni4 are antiparallel to those on Ni2 and Ni3, gives a good fit to the magnetic

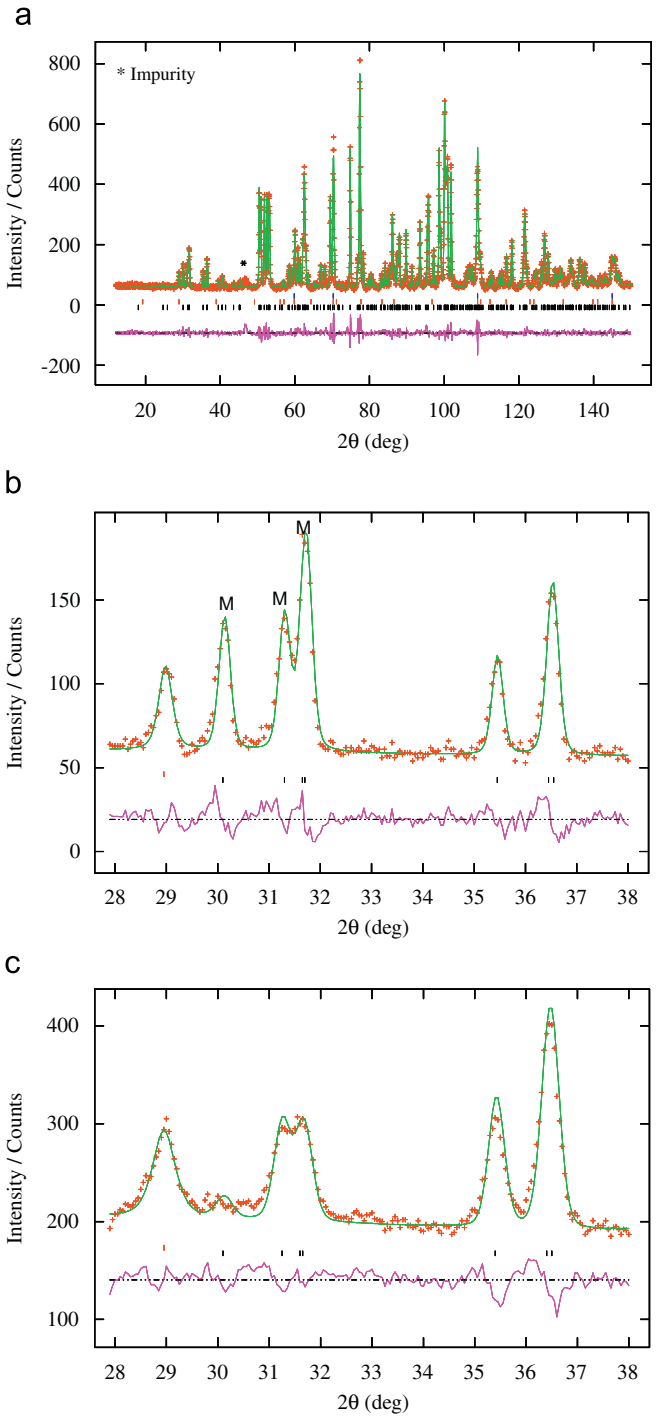

Fig. 1. Observed, calculated and difference diffraction patterns from the Rietveld analysis of the neutron powder diffraction data for $BiNiO_3$: (a) the crystal and magnetic structure fit at 5 K; (b) low angle region of the 5 K fit with magnetic peaks ($0\bar{1}1$, 011 and $101/10\bar{1}$ from left to right) labelled M; and (c) low angle region of the 300 K fit.

intensities at all measured temperatures. The 300 and 5 K fits are shown in Figs. 1(b) and (c) and the atomic parameters are given in Table 1. The refined components of the magnetic moment are shown in Table 2. The resultant moment lies close to [001] with a magnitude of 1.74(3) μ_B at 5 K, which is typical for $S=1$ Ni^{2+}, showing a slight

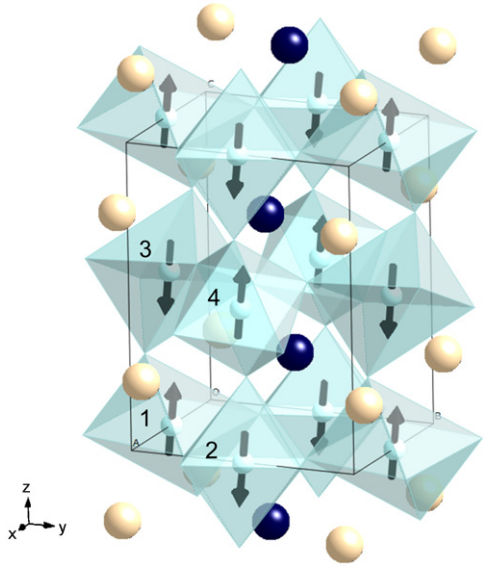

Fig. 2. Crystal and magnetic structure of $BiNiO_3$, with light and dark spheres corresponding to Bi^{3+} (site Bi1) and Bi^{5+} (Bi2), respectively, shaded NiO_6 octahedra with the inequivalent sites Ni1–Ni4 labelled, and arrows indicating the direction of the ordered magnetic moments.

Table 1
Atomic parameters for $BiNiO_3$ from the Rietveld fits to 300 K (upper values) and 5 K (lower values) powder neutron diffraction data (space group $P\bar{1}$; $a = 5.39747(7)$ Å, $b = 5.65737(8)$ Å, $c = 7.71662(11)$ Å, $\alpha = 92.179(1)^\circ$, $\beta = 89.781(1)^\circ$, $\gamma = 91.714(1)^\circ$, $V = 235.204(7)$ Å^3; $R_{wp} = 4.26\%$ and $R_{F^2} = 3.59\%$ at 300 K; $a = 5.38815(7)$ Å, $b = 5.64727(8)$ Å, $c = 7.69618(12)$ Å, $\alpha = 92.249(1)^\circ$, $\beta = 89.781(1)^\circ$, $\gamma = 91.718(1)^\circ$, $V = 233.895(7)$ Å^3; $R_{wp} = 6.41\%$ and $R_{F^2} = 4.27\%$ at 5 K)

Atom	Site	x	y	z	U_{iso} (Å^2)
Bi1	2*i*	0.0063(6)	0.0486(5)	0.2315(4)	0.0051(8)
		0.0067(8)	0.0507(6)	0.2306(5)	0.0007(10)
Bi2	2*i*	0.5105(60	0.4426(6)	0.7242(4)	0.0051(8)
		0.5097(8)	0.4430(7)	0.7230(5)	0.0007(10)
Ni1	1*d*	0.5	0	0	0.0096(6)
					0.0056(8)
Ni2	1*c*	0	0.5	0	0.0096(6)
					0.0056(8)
Ni3	1*f*	0.5	0	0.5	0.0096(6)
					0.0056(8)
Ni4	1*g*	0	0.5	0.5	0.0096(6)
					0.0056(8)
O1	2*i*	−0.1410(9)	0.4708(8)	0.2521(6)	0.0066(6)
		−0.1399(11)	0.0762(10)	0.2532(8)	0.0051(8)
O2	2*i*	0.3949(9)	0.0780(7)	0.757496)	0.0066(6)
		0.3952(11)	0.0762(9)	0.7573(7)	0.0051(8)
O3	2*i*	0.8332(8)	0.1748(7)	−0.0327(6)	0.0066(6)
		0.8353(10)	0.1745(9)	−0.0313(8)	0.0051(8)
O4	2*i*	0.3166(8)	0.3359(7)	0.0836(6)	0.0066(6)
		0.3165(11)	0.3331(9)	0.0829(8)	0.0051(8)
O5	2*i*	0.2129(8)	0.7709(7)	0.4114(6)	0.0066(6)
		0.2131(11)	0.7692(10)	0.4107(8)	0.0051(8)
O6	2*i*	0.6737(8)	0.6868(7)	0.5465(6)	0.0066(6)
		0.6734(11)	0.6859(9)	0.5459(8)	0.0051(8)

Table 2
Magnetic moment components and the resultant (μ_B), average M–O bond lengths (Å), bond valence sums (BVS)[a] and Ni–O–Ni angles (°) for $BiNiO_3$ at 5, 100, 200 and 300 K

Temperature (K)	5	100	200	300
Magnetic moments				
M_x	0.68(12)	0.95(8)	0.90(8)	0.32(20)
M_y	0.40(7)	0.25(6)	0.22(7)	0.08(22)
M_z	1.57(6)	1.42(6)	1.23(7)	0.32(21)
M	1.76(3)	1.73(2)	1.54(3)	0.49(7)
Average distances				
Bi1–O	2.848(6)	2.851(6)	2.850(6)	2.84(6)
Bi2–O	2.783(7)	2.783(6)	2.785(6)	2.788(6)
Ni1–O	2.097(6)	2.098(4)	2.099(5)	2.103(4)
Ni2–O	2.068(6)	2.067(5)	2.066(5)	2.069(4)
Ni3–O	2.085(6)	2.083(5)	2.084(5)	2.087(5)
Ni4–O	2.053(6)	2.058(5)	2.057(5)	2.063(5)
BVSs				
Bi1	3.25	3.24	3.22	3.20
Bi2	4.78	4.79	4.75	4.75
Ni1	1.83	1.83	1.83	1.81
Ni2	1.96	1.96	1.97	1.95
Ni3	1.84	1.86	1.85	1.83
Ni4	2.06	2.02	2.03	1.99
Angles				
Ni2–O1–Ni4	136.6(3)	136.6(3)	136.7(3)	136.3(3)
Ni1–O2–Ni3	139.0(3)	138.9(3)	139.0(2)	138.7(2)
Ni1–O3–Ni2	141.3(3)	141.7(2)	141.6(2)	141.6(2)
Ni1–O4–Ni2	133.7(3)	133.7(2)	133.5(2)	133.2(2)
Ni3–O5–Ni4	138.5(3)	138.4(3)	138.9(3)	138.6(3)
Ni3–O6–Ni4	143.6(3)	143.5(3)	143.8(3)	143.6(2)

[a]BVS is the sum of individual bond valences (s_i) for Bi–O and Ni–O. $s_i = \exp[(r_0 - r_i)/B]$; $B = 0.37$ Å, $r_0 = 2.094$, 2.06, 1.654 Å for Bi^{3+}–O, Bi^{5+}–O and Ni^{2+}–O, respectively.

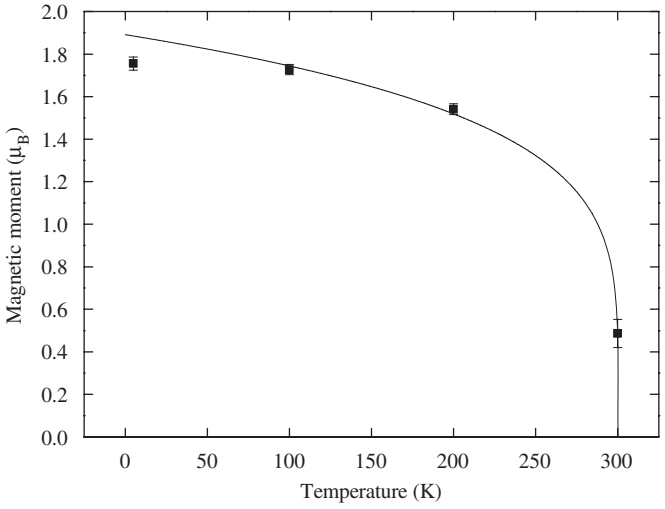

Fig. 3. Variation of the ordered Ni magnetic moment with temperature in $BiNiO_3$. A critical law curve is shown as a guide to the eye.

decrease from the ideal value of 2 μ_B due to covalency. The variation of the overall magnetic moment with temperature, shown in Fig. 3, confirms that the magnetic ordering transition temperature is very close to 300 K.

The *G*-type magnetic structure observed for $BiNiO_3$ is consistent with $3d^8$ Ni^{2+} cations at the perovskite *B*-sites, as antiferromagnetic superexchange is expected for all of the Ni–O–Ni interactions according to the Goodenough–Kanamori rules. Although the fitted magnetic model is antiferromagnetic, we note that the four Ni sites are unrelated by symmetry and so their magnetic moments will not have exactly the same orientations and magnitudes. The inexact cancellation of the opposed Ni moments results in ferrimagnetism as evidenced by the previously reported magnetic hysteresis loops [6]. However, it was not possible to refine the individual site moments against the present powder diffraction data as there were too few observed magnetic intensities. The good fit obtained with the above model shows that the deviations of the individual moments from the average are very small, and so a *G*-type antiferromagnetic model is a very good approximation to the ferromagnetic order in $BiNiO_3$.

The magnetic structure of $BiNiO_3$ is quite different to those reported for the insulating phases of the rare earth nickelate perovskites $RNiO_3$ [4,5]. Ni charge disproportionation leads to a $\sqrt{2}a_p \times \sqrt{2}a_p \times 2a_p$ superstructure of the perovskite a_p cell and a double perovskite type charge ordered arrangement, ideally $R_2Ni^{2+}Ni^{4+}O_6$, although the observed charge separation is only 30–40% of the ideal value. These phases order antiferromagnetically with a $(\frac{1}{2}0\frac{1}{2})$ magnetic propagation vector. This is typical for $A_2BB'O_6$ double perovskites with magnetic transition metals at *B* (and in some cases, *B*′) sites [13]. Competition between 90° and 180° *B*–O–*B*′–O–*B* superexchange pathways (and *B*–O–*B*′ interactions when both cations are magnetic) gives rise to complex spin ordered arrangements with $(\frac{1}{2}0\frac{1}{2})$ or $(0\frac{11}{22})$ propagation vectors. By contrast, *G*-type spin order in $BiNiO_3$ is typical for ABO_3 perovskites having non-degenerate magnetic ions at *B* sites (e.g. $RCrO_3$ and $RFeO_3$). Strong *B*–O–*B* antiferromagnetic superexchange dominates in these materials.

Comparing the structural results shows that no crystallographic phase transition occurs in the range 5–300 K and the triclinic structure hardly changes throughout (Table 2). The unit cell lengths *a*, *b* and *c* all decrease slightly with temperature, but there is no discontinuity in the thermal variation of the structural parameters (Fig. 4). The 300 K structure refinement is very similar to those reported previously using X-ray [6] and neutron [7] diffraction. The bond valence sums, BVS [14], in Table 2 confirm a very high degree (78%) of Bi charge disproportionation. The BVS at 5 K are almost identical to those at 300 K, showing that the charge distribution remains $Bi^{3+}_{0.5}Bi^{5+}_{0.5}Ni^{2+}O_3$ down to 5 K. It was recently proposed that four distinct charge distributions should be observable in $BiNiO_3$ [7]. The pressure-induced transition from insulating, Bi-disproportionated $Bi^{3+}_{0.5}Bi^{5+}_{0.5}Ni^{2+}O_3$ to metallic $Bi^{3+}Ni^{3+}O_3$ was confirmed by neutron diffraction, and stabilised forms of the $Bi^{4+}Ni^{2+}O_3$ state with La [9] or Pb [15] partly substituted for Bi have also been prepared. The fourth possibility, Ni-disproportionated $Bi^{3+}Ni^{2+}_{0.5}Ni^{4+}_{0.5}O_3$, has not yet been observed, and the present study demonstrates that it is not formed at ambient pressure down to 5 K. High pressures and low temperatures, and perhaps substitution of Bi by smaller rare earth cations, may be needed to stabilise the Ni-disproportionated phase.

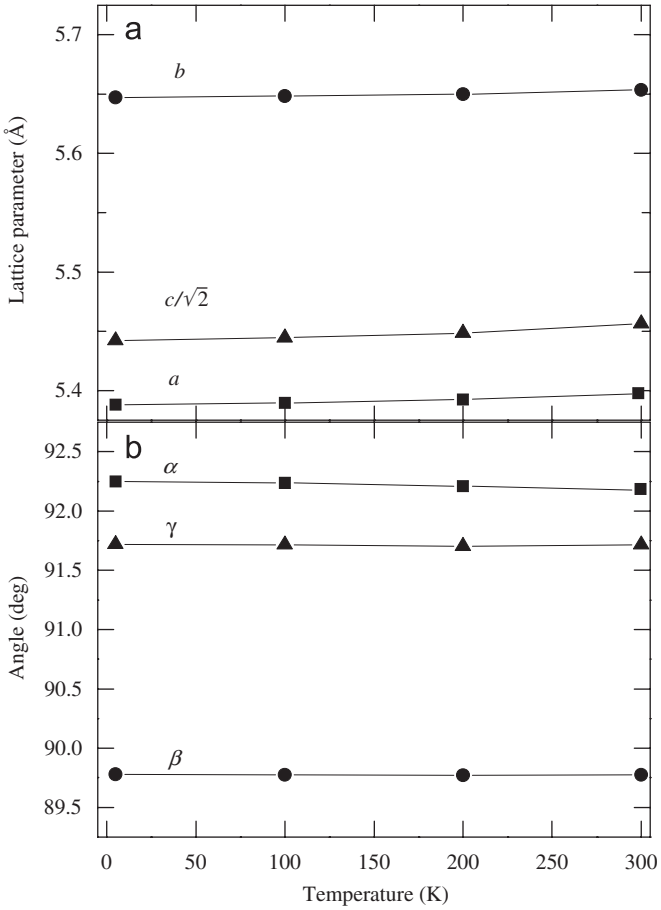

Fig. 4. Temperature dependence of unit-cell lengths (a) and angles (b) for $BiNiO_3$.

Acknowledgments

We thank EPSRC and the Leverhulme Trust for support.

References

[1] J.B. Torrence, P. Lacorre, A.I. Nazzal, E.J. Ansaldo, C.H. Niedermayer, Phys. Rev. B 45 (1992) 8209.
[2] M.L. Medarde, J. Phys.: Condens. Matter 9 (1997) 1679.
[3] J.L. Garcia-Muñoz, J. Rodriguez-Carvajal, P. Lacorre, J.B. Torrance, Phys. Rev. B 46 (1992) 4414.
[4] J.L. Garcia-Muñoz, J. Rodriguez-Carvajal, P. Lacorre, Phys. Rev. B 50 (1994) 978.
[5] J. Rodriguez-Carvajal, S. Rosenkranz, M. Medarde, P. Lacorre, M.T. Frenandez-Diaz, F. Fauth, V. Trounov, Phys. Rev. B 57 (1998) 456.
[6] S. Ishiwata, M. Azuma, M. Takano, E. Nishibori, M. Takata, M. Sakata, K. Kato, J. Mater. Chem. 12 (2002) 3733.

[7] M. Azuma, S. Carlsson, J. Rodgers, M.G. Tucker, M. Tsujimoto, S. Ishiwata, S. Isoda, Y. Shimakawa, M. Takano, J.P. Attfield, J. Am. Chem. Soc. 129 (2007) 14433.
[8] S. Ishiwata, M. Azuma, M. Takano, Solid State Ionics 172 (2004) 569.
[9] S. Ishiwata, M. Azuma, M. Hanawa, Y. Morimoto, Y. Ohishi, K. Kato, M. Takata, E. Nishibori, M. Sakata, I. Terasaki, M. Takano, Phys. Rev. B 72 (2005) 045104.
[10] H. Wadati, M. Yakizawa, T.T. Tran, K. Tanaka, T. Mikozawa, A. Fujumori, A. Chikamatsu, H. Kumigashira, M. Oshima, S. Ishiwata, M. Azuma, M. Takano, Phys. Rev. B 72 (2005) 155103.
[11] H.M. Rietveld, J. Appl. Crystallogr. 2 (1969) 65.
[12] A.C. Larson, R.B. Von Dreele, Los Alamos National Laboratory Report No. LAUR 86-748, 1994 (unpublished).
[13] J.-W.G. Bos, J.P. Attfield, Phys. Rev. B 70 (2004) 174434.
[14] N.E. Brese, M. O'Keefe, Acta Crystallogr. Sect. B 47 (1991) 192.
[15] S. Ishiwata, M. Azuma, M. Takano, Chem. Mater. 19 (2007) 1964.